



Studies in *Gyromitra* I: the *Gyromitra gigas* species complex

Andrew N. Miller¹ · Angela Yoon² · Gro Gulden³ · Øyvind Stensholt³ · Nicolas Van Vooren⁴ · Esteri Ohenoja⁵ · Andrew S. Methven⁶

Received: 18 August 2020 / Revised: 8 October 2020 / Accepted: 12 October 2020

© German Mycological Society and Springer-Verlag GmbH Germany, part of Springer Nature 2020

Abstract

The *Gyromitra gigas* species complex includes six morphologically similar taxa, several of which have a long history of segregation, synonymization, and rearrangement among different genera. These taxa occur throughout Asia, Europe, and North America and include *G. gigas*, *G. khanspurensis*, *G. korfii*, *G. montana*, *G. pseudogigas*, and *G. ticiniana*. ITS and LSU sequences from 66 specimens, including type specimens for all six taxa, were included in phylogenetic analyses to establish species boundaries and resolve species relationships. Sequence similarity comparisons were also conducted between the two molecular markers and between the ITS1 and ITS2 regions. Although ITS exhibited sufficient variability to discriminate among species in the *G. gigas* species complex, LSU displayed very low variability rendering it completely useless as a molecular marker for separating taxa in this group. The ITS1 region was twice as informative as the ITS2 region and can be used as a barcode marker to identify these species. *Gyromitra gigas* and *G. montana* occur as a well-supported clade of sister species and can be distinguished based on ascospore morphology. *Gyromitra korfii* and *G. ticiniana* also form a highly supported clade and are considered distinct species based on geography. *Gyromitra littiniana* is confirmed to be synonymous with *G. ticiniana* based on molecular data. *Gyromitra khanspurensis* and *G. pseudogigas*, which also form a highly supported clade, are considered separate species early in the process of speciation that differ significantly in ascomata and ascospore morphology. A key to species based on morphology and geography is provided.

Keywords Ascomycota · Fungi · Holotype barcoding · ITS sequences · Systematics

Introduction

The genus *Gyromitra* Fr. contains over 70 taxa commonly referred to as false morels. Members are distributed primarily throughout north temperate and boreal regions of the Northern

Hemisphere and form stipitate to sessile ascomata with discoid to cerebriform or saddle-shaped apothecia mostly during the spring. *Gyromitra* taxa have a long, complex taxonomic history of transfers among various genera (e.g., *Discina*, *Helvella*, *Maublancomyces*, *Neogyromitra*, and *Pseudorhizina* among others), re-segregation into multiple subgenera, and repeated splitting and recombining of taxa at the species level and below. The history and taxonomy of *Gyromitra* and its segregates have been summarized by numerous authors (Donadini 1984, 1986; Harmaja 1969, 1973; McKnight 1969, 1971, 1973; Van Vooren and Moreau 2009a, 2009b, 2009c).

Based on previous phylogenetic studies (Methven et al. 2013; Miller et al. 2015; Krisai-Greilhuber et al. 2017; Carbone et al. 2018; Wang and Zhuang 2019), six taxa can be included in the *G. gigas* species complex: *G. gigas* (Krombh.) Quél., *G. khanspurensis* Jabeen and Khalid, *G. korfii* (Raitv.) Harmaja, *G. montana* Harmaja, *G. pseudogigas* X.C. Wang and W.Y. Zhuang, and *G. ticiniana* Littini. Although other taxa, such as *G. grandis* (Cumino) Van Vooren and M. Carbone (syn. *G. fastigiata* (Krombh.) Rehm), *G. leucoxantha* (Bres.) Harmaja,

Section Editor: Roland Kirschner

✉ Andrew N. Miller
amiller7@illinois.edu

¹ Illinois Natural History Survey, University of Illinois Urbana-Champaign, Champaign, IL, USA

² Department of Molecular and Cellular Biology, University of Illinois Urbana-Champaign, Champaign, IL, USA

³ Natural History Museum, University of Oslo, Oslo, Norway

⁴ Tassin-la-Demi-Lune, France

⁵ Botanical Museum, Biodiversity Unit, University of Oulu, Oulu, Finland

⁶ Savannah, GA, USA

G. perlata (Fr.) Harmaja, and *G. slonevskii* Heluta, appear as closely related sister taxa in some of the previous studies, their ITS sequences are far too divergent and do not occur within a well-supported clade with members of the *G. gigas* species complex.

Gyromitra gigas is a common, widespread European taxon, first described by Krombholtz (1834) as *Helvella gigas* based on a specimen collected in the Czech Republic. Although the color illustration that accompanies the description serves as the lectotype (MBT 383599), this species was recently epitypified (MBT 383600) with a specimen from the Czech Republic that was sequenced for the ITS and LSU (Carbone et al. 2018). The European name, *G. gigas*, has been frequently used for North American material although two other names have been proposed to accommodate specimens from eastern (*G. korfii*) and western/northern (*G. montana*) areas of North America.

Gyromitra korfii was originally described by Raitviir (1970) as *Discina korfii* based on the considerably more slender ascospores than those of *G. gigas*. Raitviir (1970) noted “No true *N.[eogyromitra] gigas* from North America could be found” among the specimens he examined from CUP. This taxon was later transferred to *Gyromitra* by Harmaja (1973), who further distinguished it from *G. gigas* based on its shorter ascospores, more delicate ascospore ornamentation, and broader apices of the paraphyses.

Harmaja (1973) subsequently described a new species, *G. montana*, based on a specimen identified as *G. gigas* by McKnight (1971) from WY, USA. Harmaja distinguished *G. montana* from *G. gigas* and *G. korfii* based on subtle differences in ascospore shape, size, ornamentation, presence, and length of apiculi and broader tips of the paraphyses. In their review of the Helvellaceae, Abbott and Currah (1997) considered *G. korfii* and *G. montana* as synonyms under *G. gigas*. Although Methven et al. (2013) did not include *G. gigas* in their phylogenetic analysis, they treated *G. montana* as a synonym of *G. korfii*. Miller et al. (2015) later raised the possibility that all three taxa could be distinct species.

Gyromitra ticiniana was described by Littini (1988) from Italy without discussing how it differed from *G. gigas*. Riva (1998, 2010) in a later examination of this species (as *G. littiniana* Riva) concluded that it could be distinguished from *G. gigas* by its growth in deciduous forests (vs. coniferous forests in *G. gigas*) and narrower ascospores with finer ornamentation. Carbone et al. (2018) explained why *G. littiniana* was a superfluous name and, thus, a later synonym of *G. ticiniana*. Since attempts to sequence the holotype of *G. ticiniana* were unsuccessful, Carbone et al. (2018) designated an epitype (MBT 383602) from which they obtained ITS and LSU sequences based on an Italian collection matching the ecological and morphological concept of *G. ticiniana*.

Gyromitra khanspurensis was recently described from Pakistan by Jabeen and Khalid (Krisai-Greilhuber et al. 2017) who distinguished it from *G. gigas* and *G. korfii* by its smaller ascospores with a short apiculus and from *G. korfii* by its more convoluted hymenium and smooth stalk. The ITS was sequenced for *G. khanspurensis* and it differed compared to the single included ITS sequence (JF908781) of *G. gigas* from Italy.

Lastly, *G. pseudogigas* was described from China by Wang and Zhuang (2019) based on a 3-gene phylogeny (ITS, LSU, and *TEF-1*) which included three representatives of *G. gigas* from China, France, and Italy and a single representative of *G. ticiniana* from Turkey. They distinguished *G. pseudogigas* from *G. gigas* based on its saddle-shaped apothecia and finely roughened rather than reticulate ascospores.

Although previous studies included one or more of these taxa in molecular phylogenetic analyses (Methven et al. 2013; Miller et al. 2015; Krisai-Greilhuber et al. 2017; Carbone et al. 2018; Wang and Zhuang 2019), no study to date has comprehensively analyzed all of the taxa in the *G. gigas* species complex or assessed the ITS and LSU as barcode markers for identifying these taxa. The goals of this study were to sample and sequence multiple representatives, including type specimens, for all six taxa in the *G. gigas* species complex to establish species boundaries, resolve species relationships, and assess the potential of ITS and LSU as barcode markers.

Materials and methods

Specimens examined

Entire dried ascomata or small portions of the fertile layer of ascomata were sent to the first author either as loans or gifts. Sequences generated during this study were obtained from DNA extracted directly from these dried ascomata, which were deposited at ILLS or available at their home institution (BPI, CUP, DAOM, ILLS, LUG, O, OSC, OULU, NY, TAAM, WTU, and YSU). Fungarium acronyms follow Index Herbariorum (Thiers 2013). Efforts were made to generate sequences from the type specimens for *G. korfii*, *G. littiniana*, and *G. montana* even though they date from 1953, 2010, and 1967, respectively. Although the holotype specimen of *G. korfii* (CUP-K-4801) was previously “lost,” it was recently discovered in an old box of Korf specimens at CUP (Teresa Iturriaga pers. comm.). However, the entire collection consists of mostly soil debris with a few scattered remains of what was assumed to be an ascoma of *G. korfii* (see record at MyCoPortal 2020). One of these small fragments was used for DNA extraction and the ITS1 region was successfully sequenced. The isotype of *G. montana*, which consists of several ascomata in good condition, was

obtained from BPI and successfully sequenced for the ITS and LSU. Finally, a small fragment of the holotype of *G. littiniana* was obtained from LUG and successfully sequenced for ITS and LSU.

Micromorphological features were studied and measurements made of material revived in 95% ethanol and distilled water, sectioned, and then mounted in distilled water (McKnight 1968) or lactophenol cotton blue. Sections were examined with a light microscope at $\times 400$ and $\times 1000$. A minimum of 25 ascospores and paraphyses were measured for each collection. In addition to assembling a range of ascospore lengths and widths for each specimen, the mean length (L_m), mean width (W_m), length-width ratio (Q), and mean length-width ratio (Q_m) were calculated for each specimen. The following specimens were examined and annotated: *G. gigas* (ILLS00121401, ILLS00121405 (immature), ILLS00121415, O174609 (immature)), *G. korffii* (CUP 58839, ILLS00114754), *G. montana* (ILLS00114753, ILLS00121414, ILLS00121419 (immature), ILLS00165101, ILLS00165152), and *G. ticiniana* (ILLS00121412, ILLS00121413 (isoeotype)). Voucher specimen number, locality, GenBank accession numbers, and source for all taxa included in the ITS and LSU analyses are shown in Table 1.

Since the ascomata develop and mature over an extended period of time, the apothecia often produce ascospores that vary widely in length and width as well as the development of surface ornamentation and the apiculi. For the purposes of this study, the apiculi are included in the measurements of ascospore length. However, it is unclear in the literature whether or not the apiculi have been consistently included in the measurements of ascospore lengths. Ascospore maturity and inclusion/exclusion of the apiculi in the ascospore length may account for the diverse ranges of surface ornamentation and ascospore lengths and widths reported in the literature.

Molecular data

DNA was extracted directly from dried ascomata using either a modified NaOH extraction method (Osmundson et al. 2013) or an E.Z.N.A.® Microelute Genomic DNA kit (Omega Biotek, Norcross, GA, USA) following the manufacturer's instructions. For NaOH extraction, 200 μ L 0.5 M NaOH was added to ~ 75 mg of dried tissue, ground with a micropestle, centrifuged at 14000 RPM for 2 min, and 5 μ L of the resulting supernatant added to 495 μ L 100 mM Tris-HCl buffered with NaOH to pH 8.5–8.9 (Tris-HCl-DNA extraction solution). The complete internal transcribed spacer (ITS) region and the first 1100 bp of the 5' end of 28S nuclear ribosomal large subunit (LSU) were amplified separately. PCR amplification using a GoTaq® Green Master mix (Promega, Madison, WI, USA) consisted of the following: 12.5 μ L GoTaq® Green Master mix, 2.5 μ L BSA, 2.5 μ L 50% DMSO, 2 μ L of each 10 μ M primer ITS1F/ITS4 or LROR/LR6, and 3–7 μ L DNA.

PCR amplification was completed on a Bio-Rad PTC 200 thermal cycler under the following parameters: initial denaturation at 94 °C for 2 min, followed by 40 cycles of 94 °C for 30 s, 47 °C for 45 s, 72 °C for 1 min with a final extension step of 72 °C for 10 min. If PCRs failed to amplify, then puReTaq™ Ready-To-Go PCR Beads (GE Healthcare, Chicago, IL, USA) were used in place of the GoTaq® Green Master mix as above according to the manufacturer's instructions. Gel electrophoresis (1% TBE agarose gel stained with ethidium bromide) was used to verify the presence of a PCR product. PCR products were purified using a Wizard® SV Gel and PCR Clean-Up System (Promega, Madison, WI, USA), and template DNA was used in 10 μ L sequencing reactions with BigDye® Terminator v3.1 (Applied Biosystems, Foster City, CA, USA) using a combination of the following primers: ITS1F, ITS2, ITS3, ITS4, LROR, LR3, LR3R, and LR6 (Gardes and Bruns 1993; Rehner and Samuels 1995; Vilgalys and Hester 1990; White et al. 1990). Sequences were generated on an Applied Biosystems 3730XL high-throughput capillary sequencer at the W.M. Keck Center at the University of Illinois Urbana-Champaign. Consensus ITS and LSU sequences were assembled with Sequencher 5.4 (Gene Codes Corp., Ann Arbor, MI, USA).

Phylogenetic analyses

The ITS and LSU datasets were individually aligned using the MUSCLE® multiple alignment program as implemented in Sequencher 5.4 and the ITS alignment was manually corrected by eye. Final ITS and LSU alignments are deposited in TreeBase (26774). The LSU alignment was rooted with *G. leucoxantha* based on previous analyses (Methven et al. 2013). The ITS alignment was rooted with *G. khanspurensis* and *G. pseudogigas* based on the LSU tree since rooting with *G. leucoxantha* considerably increased the amount of ambiguity in the highly variable ITS alignment. Portions of the 5' and 3' ends of the ITS dataset were excluded from all analyses due to missing data in most taxa. Ambiguously aligned regions were removed from the final alignments using Gblocks (Castresana 2000; Talavera and Castresana 2007), employing the less stringent parameters. The best-fit model of evolution for both datasets was determined to be the general time reversible (GTR) model (Rodríguez et al. 1990) by jModeltest (Darriba et al. 2012; Guindon and Gascuel 2003) based on the Akaike information criterion (AIC) (Posada and Buckley 2004). A maximum likelihood (ML) analysis with 1000 bootstrap replicates was performed using PhyML as implemented in Seaview 4.7 (Gouy et al. 2010), with all parameters optimized and the GTR model. A ML analysis with 1000 bootstrap replicates was also performed using RAXML-HPC2 v.8.2.12 (Stamatakis 2014) with a GTRCAT approximation using the CIPRES Science Gateway v.3.3 portal (Miller et al. 2010). Bootstrap replicates were performed

Table 1 Specimens used in this study including type status, voucher specimen number, locality, ITS and LSU GenBank accession numbers and source of sequences

Species	Voucher specimen no.	Locality	ITS GenBank no.	LSU GenBank no.	Source
<i>Gyromitra gigas</i> Epitype	TUR-A 208088	Czech Republic	MH938663	MH938309	Carbone et al. 2018
	TUR-A 208089	Italy	MH938666	---	Carbone et al. 2018
	TUR-A 208091	Italy	MH938667	MH938312	Carbone et al. 2018
	TUR-A 208092	Italy	MH938668	MH938313	Carbone et al. 2018
	TUR-A 208093	Italy	MH938669	MH938314	Carbone et al. 2018
	14754	Italy	JF908781	---	Osmundson et al. 2013
	TAAMI190163	Estonia	MW076963	MW076976	This study
	TU117077	Estonia	UDB020355	UDB020355	Tedersoo et al.
	G4178	Estonia	UDB0485039	---	Tedersoo et al.
	G4382	Estonia	UDB0435061	---	Tedersoo et al.
	G4390	Estonia	UDB0466718	---	Tedersoo et al.
	G4510	Estonia	UDB0392834	---	Tedersoo et al.
	G4626	Estonia	UDB0327095	---	Tedersoo et al.
	G4627	Estonia	UDB0337494	---	Tedersoo et al.
	G4768	Estonia	UDB0483315	---	Tedersoo et al.
	G4813	Estonia	UDB0192402	---	Tedersoo et al.
	O174609	Norway	MW076964	KX008328	This study
	O174628	Norway	MW076965	KX008329	This study
	O174629	Norway	MW076966	KX008330	This study
	H.546	Turkey	KX420694	---	Gungor et al. unpublished
H.559	Turkey	KX420695	---	Gungor et al. unpublished	
H.815	Turkey	KX420696	---	Gungor et al. unpublished	
LK95 04 08	Hungary	MH938664	MH938310	Carbone et al. 2018	
OULU-F 23717; ILLS00121402	Finland	MW076967	MW076977	This study	
OULU-F 23577; ILLS00121403	Finland	---	MW076978	This study	
OULU-F 25304; ILLS00121404	Finland	---	MW076979	This study	
OULU-F 25301; ILLS00121405	Finland	MW076968	MW076980	This study	
LY NV 2007.04.20	France	MH938665	MH938311	Carbone et al. 2018	
HMAS254604; ILLS00121400	France	MG846996	MG847005	Wang and Zhuang 2019	
ILLS00121401	France	MW076969	MW076969	This study	
ILLS00121407	France	MW076970	MW076970	This study	
ILLS00121408	France	MW076971	MW076971	This study	
ILLS00121409	France	MW076972	---	This study	

Table 1 (continued)

Species	Voucher specimen no.	Locality	ITS GenBank no.	LSU GenBank no.	Source
<i>Gyromitra khanspurensis</i>	ILLS00121410	France	MW076973	---	This study
	ILLS00121411	France	MW076974	MW076974	This study
	HMAS89008	China: Jilin	MG846995	MG847004	Wang and Zhuang 2019
	YSU-F-08006; ILLS00121415	Russia: Khanty-Mansiyskiy	MW076975	MW076981	This study
	L.AH35074	Pakistan	NR156340 (MF116159)	---	Krisai-Greilhuber et al. 2017
<i>Gyromitra korfii</i>	CUP 2631	USA: New York	MW075384	---	This study
	CUP 28997	USA: North Carolina	MW075385	MW078425	This study
	NY 01797011	USA: Pennsylvania	---	KC751513	Methven et al. 2013
	FH 567158	USA: Massachusetts	MW075386	---	This study
	NY 01797010	USA: Illinois	MW075387	KC751511	This study, Methven et al. 2013
	NY 01293395	USA: Illinois	---	KC751499	Methven et al. 2013
	NY 01797009	USA: Michigan	---	KC751519	Methven et al. 2013
	NY 01797012	USA: Michigan	MW075389	KC751506	This study, Methven et al. 2013
	NY 01797013	USA: Michigan	---	KC751510	Methven et al. 2013
	ILLS00114754	USA: Michigan	MW075390	MW078426	This study
<i>Gyromitra leucoxantha</i>	NY 03817715	USA: Missouri	MW075391	MW078427	This study
	ILLS00121418	Andorra	MW078428	MW078428	This study
<i>Gyromitra litinitiana</i>	TAAM 145678	Austria: Tyrol	---	KX185091	Miller et al. 2015
	LUG 14130	Italy	MW075392	MW078429	This study
<i>Gyromitra montana</i>	BPI 566707	USA: Wyoming	MW077452	MW077442	This study
	ILLS00165101	USA: California	MW077453	KC751518	This study, Methven et al. 2013
	OSC 138696	USA: California	MW077454	MW077443	This study
	WTU-F-016534; ILLS00121414	USA: Washington	MW077455	---	This study
Labeled as <i>G. korfii</i>	JLF3797	USA: Oregon	MK834667	---	J.L. Frank unpublished
	NY 01797008	USA: Colorado	MW077456	KC751512	This study, Methven et al. 2013
	ILLS00114753	USA: Colorado	MW077457	MW077444	This study
	AN 043490; MO277111	USA: Arizona	MN176988	MN203622	T.A. Clements unpublished
	ILLS00165152	USA: Michigan	MW077458	---	This study
	DAOM 706056; ILLS00121424	Canada: Newfoundland	MW077459	MW077445	This study

Table 1 (continued)

Species	Voucher specimen no.	Locality	ITS GenBank no.	LSU GenBank no.	Source
<i>Gyromitra pseudogigas</i>	DAOM 706057; ILLS00121420	Canada: Newfoundland	MW077460	MW077446	This study
	DAOM 706058; ILLS00121421	Canada: Newfoundland	MW077461	MW077447	This study
	DAOM 706059; ILLS00121422	Canada: Newfoundland	MW077462	MW077448	This study
	DAOM 706060; ILLS00121423	Canada: Newfoundland	MW077463	MW077449	This study
	DAOM 706061; ILLS00121419	Canada: Newfoundland	MW077464	MW077450	This study
Holotype	HMAS46539	China: Sichuan	MG846994	MG847023	Wang and Zhuang 2019
<i>Gyromitra ticiniana</i>	TUR-A 208095	Italy	MH938672	MH938317	Carbone et al. 2018
	TUR-A 208096	Italy	MH938673	MH938318	Carbone et al. 2018
	TUR-A 208097	Italy	MH938674	MH938319	Carbone et al. 2018
	TUR-A 208094	Italy	MH938671	MH938316	Carbone et al. 2018
	H.373	Turkey	KX420699	---	Gungor et al. unpublished
	ILLS00121412	France	MH938670	MH938315	Carbone et al. 2018

1000 times under the GTR model employing GAMMA model of rate heterogeneity and the rapid bootstrapping option (Stamatakis et al. 2008). Clades with bootstrap values (BV) $\geq 70\%$ were considered significant and strongly supported (Hillis and Bull 1993). Bayesian analyses were performed using MrBayes v 3.2.7 (Huelsenbeck and Ronquist 2001, 2005) under the above model on the CIPRES 3.3 portal. Constant characters were included and 10 million generations with trees sampled every 1000th generation were run, resulting in 10,000 total trees. The first 2500 trees were discarded as burn-in, and Bayesian posterior probabilities (BPP) were determined from a consensus tree generated from the remaining 7500 trees using PAUP* v.4.0a (build 166) (Swofford 2002). Clades with BPP $\geq 95\%$ were considered significant and strongly supported (Alfaro et al. 2003; Larget and Simon 1999).

Sequence similarity comparisons

The ITS alignment was subjected to further analysis to assess the utility of the official fungal barcode in this group (Schoch et al. 2012). Distance analysis set to uncorrected “p” was used in PAUP* v.4.0a (build 166) (Swofford 2002) to calculate the mean and range for infraspecific and interspecific variation. Intraspecific variation could not be calculated for *G. khanspurensis* and *G. pseudogigas* since each was represented by a single sequence. Similar analyses were performed with the LSU alignment and comparisons were made between the ITS1 and ITS2 regions, which were delimited using the ITSx program in PlutoF (Abarenkov et al. 2010).

Results

Phylogenetic analyses

PCR amplification and Sanger sequencing of ITS and LSU were largely successful for most specimens, even those 30–70 years old (Table 1). PCR amplification of *TEF-1* failed for several recent specimens so no further attempts were made to include this gene in our analyses. The final ITS alignment of 66 sequences consisted of 710 nucleotides after the removal of 42 nucleotides representing ambiguous regions. The ITS contained 140 parsimony-informative characters, 95 in the ITS1 region and 45 in the ITS2 region.

The final LSU alignment of 51 sequences consisted of 1127 nucleotides. No ambiguous regions were present in the LSU dataset. The LSU contained only 17 parsimony-informative characters and lacked sufficient phylogenetic signal to differentiate among *G. gigas*, *G. korfii*, *G. montana*, and *G. ticiniana* (data not shown) so phylogenetic relationships are based only on the ITS dataset.

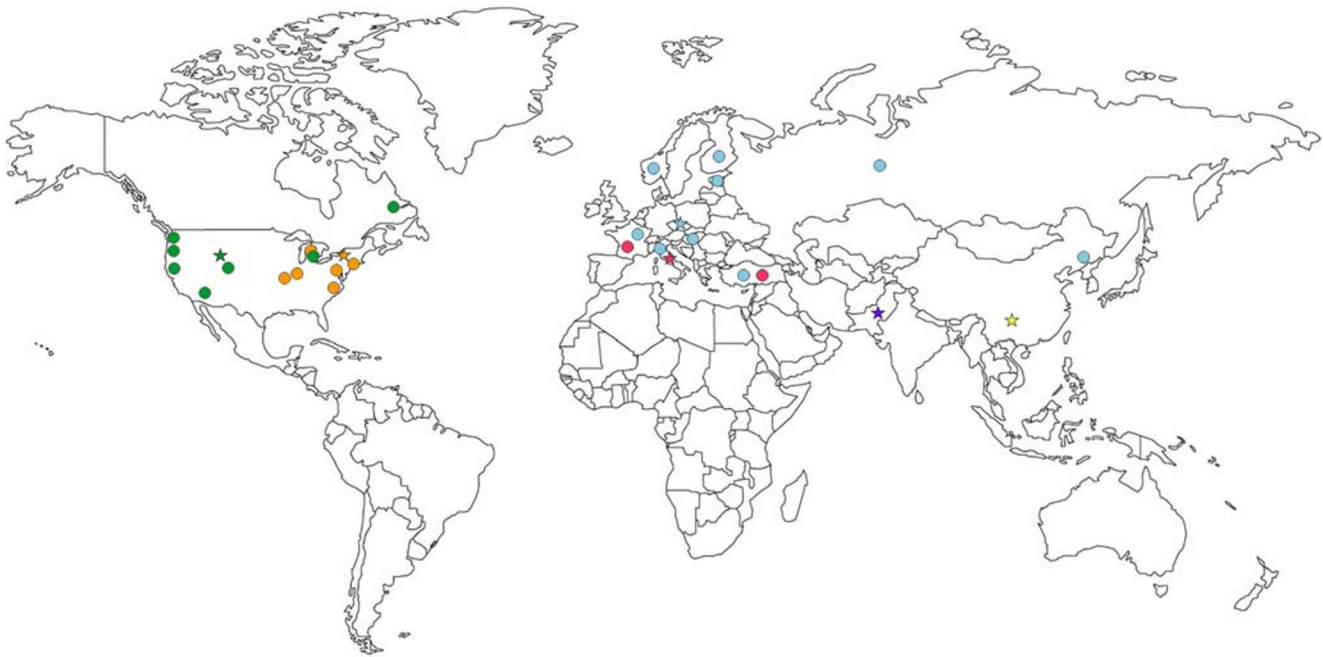


Fig. 2 Distribution map for all specimens in the *G. gigas* species complex sequenced in this study. Type specimens for each species are shown as stars and voucher specimens are shown as circles. Colors for each species correspond to those used in Fig. 1

LSU sequence variation on average was zero in *G. ticiniana*, 0.05% in *G. gigas*, 0.1% in *G. montana*, and 0.4% in *G. korfii*. Interspecific ITS sequence variation on average ranged from 0.6% between *G. khanspurensis* and *G. pseudogigas* to 17.4% between *G. gigas* and *G. korfii*. Interspecific LSU sequence variation on average ranged from 0.3% between *G. korfii* and *G. ticiniana* to 1.6% between *G. montana* and *G. pseudogigas*. Intraspecific variation averaged less than 0.4% for all species comparisons for both ITS and LSU, whereas ITS interspecific variation averaged more than 5.9% for all species comparisons except for *G. khanspurensis*/*G. pseudogigas* and *G. korfii*/*G. ticiniana*.

Interspecific variation in LSU averaged below 1.6% for all species comparisons.

The two regions of ITS were compared to investigate whether only one region (i.e., either ITS1 or ITS2) could be used for molecular identification of these taxa (Table 3). The ITS1 region contained more than twice the number of parsimony-informative characters compared to the ITS2 region (95 vs. 45) so it was expected that, in general, the ITS1 would vary twice as much as the ITS2. Intraspecific ITS1 sequence variation on average was zero in *G. ticiniana*, 0.2% in *G. gigas*, 0.3% in *G. korfii*, and 0.6% *G. montana*. Intraspecific ITS2 sequence variation on average was zero in

Table 2 Intraspecific and interspecific sequence variation of the ITS and LSU for specimens in the *G. gigas* species complex. Mean and range (in parentheses) of percent differences based on uncorrected “p” sequence differences are shown for ITS along the upper diagonal and for LSU along the lower diagonal. Intraspecific variation could not be calculated for *G. khanspurensis* and *G. pseudogigas* since each species was represented by a single sequence. No LSU sequence exists for *G. khanspurensis*

	<i>G. gigas</i>	<i>G. khanspurensis</i>	<i>G. korfii</i>	<i>G. montana</i>	<i>G. pseudogigas</i>	<i>G. ticiniana</i>
<i>G. gigas</i>	ITS = 0.2 (0 – 1.1) LSU = 0.05 (0 – 0.3)	15.7 (15.4 – 22.3)	17.4 (15.6 – 25.3)	5.9 (3.8 – 8.3)	15.1 (14.8 – 21.4)	15.5 (15.0 – 21.7)
<i>G. khanspurensis</i>	N/A	N/A	7.3 (6.4 – 11.0)	15.3 (10.9 – 15.8)	0.6 (N/A)	6.4 (6.2 – 6.5)
<i>G. korfii</i>	0.6 (0 – 1.4)	N/A	ITS = 0.4 (0 – 1.0) LSU = 0.4 (0 – 1.4)	15.8 (10.7 – 22.3)	7.4 (6.5 – 11.2)	1.7 (1.2 – 2.9)
<i>G. montana</i>	0.4 (0.2 – 0.8)	N/A	0.6 (0 – 1.4)	ITS = 0.4 (0 – 1.2) LSU = 0.1 (0 – 0.3)	14.4 (10.3 – 14.9)	14.8 (10.7 – 15.6)
<i>G. pseudogigas</i>	1.1 (1.0 – 1.5)	N/A	1.3 (1.1 – 1.7)	1.6 (1.5 – 1.9)	N/A	6.4 (6.2 – 6.5)
<i>G. ticiniana</i>	0.7 (0.5 – 1.1)	N/A	0.3 (0 – 1.1)	0.9 (0.8 – 1.2)	1.1 (1.0 – 1.2)	ITS = 0 LSU = 0

Table 3 Intraspecific and interspecific sequence variation of the ITS1 and ITS2 regions for specimens in the *G. gigas* species complex. Mean and range (in parentheses) of percent differences based on uncorrected “p” sequence differences are shown for ITS1 along the upper diagonal

	<i>G. gigas</i>	<i>G. khanspurensis</i>	<i>G. korfii</i>	<i>G. montana</i>	<i>G. pseudogigas</i>	<i>G. ticiniana</i>
<i>G. gigas</i>	ITS1 = 0.2 (0–1.5)	26.2 (26.1–26.5)	25.9 (25.8–26.4)	8.8 (5.3–10.1)	25.2 (25.1–25.5)	25.4 (25.2–25.5)
	ITS2 = 0.3 (0–1.9)					
<i>G. khanspurensis</i>	12.3 (11.8–12.7)	N/A	10.7 (10.3–11.3)	23.9 (15.6–25.5)	1.1 (N/A)	10.1 (9.8–10.5)
<i>G. korfii</i>	13.9 (12.7–15.2)	6.8 (6.2–7.5)	ITS1 = 0.3 (0–1.0)	21.5 (13.9–23.1)	11.1 (10.8–11.7)	3.1 (2.8–3.1)
			ITS2 = 0.7 (0–1.8)			
<i>G. montana</i>	4.0 (3.2–5.1)	13.2 (12.7–13.6)	15.2 (13.3–16.8)	ITS1 = 0.6 (0–2.2)	22.3 (14.1–23.6)	21.8 (13.9–22.8)
				ITS2 = 0.4 (0–1.4)		
<i>G. pseudogigas</i>	11.8 (11.3–12.2)	0.5 (N/A)	6.3 (6.1–7.0)	12.7 (12.1–13.2)	N/A	10.6 (10.2–10.9)
<i>G. ticiniana</i>	12.9 (12.0–13.7)	6.4 (6.1–6.6)	0.5 (0–1.8)	14.3 (13.3–15.8)	5.9 (5.7–6.1)	ITS1 = 0
						ITS2 = 0

G. ticiniana, 0.3% in *G. gigas*, 0.4% in *G. montana*, and 0.7% in *G. korfii*. Interspecific ITS1 sequence variation on average ranged from 1.1% between *G. khanspurensis* and *G. pseudogigas* to 26.2% between *G. gigas* and *G. khanspurensis*. Interspecific ITS2 sequence variation on average ranged from 0.5% between *G. korfii* and *G. ticiniana* and between *G. khanspurensis* and *G. pseudogigas* to 15.2% between *G. korfii* and *G. montana*. Intraspecific variation averaged less than 0.7% for all species comparisons, whereas interspecific variation averaged more than 3% for all species comparisons except for *G. khanspurensis*/*G. pseudogigas* in ITS1 and ITS2 and *G. korfii*/*G. ticiniana* in ITS2.

Species concepts

Species within the *G. gigas* species complex are characterized by stipitate ascomata, apothecia that are saddle-shaped to irregularly lobed or cerebriform and wrinkled, and yellow-brown to brown to reddish brown, ribbed to sulcate, white to yellow-brown stipe, ellipsoid to fusiform ascospores that are roughened to finely reticulate and uniguttulate or triguttulate with an inconspicuous to distinctive apiculus that is up to 4 μm long. While the majority of the taxa in this species complex have convoluted to cerebriform apothecia, *G. pseudogigas*, known only from China, is distinguished from the other taxa by its saddle-shaped apothecia. *Gyromitra khanspurensis*, reported only from Pakistan, has distinctly smaller ascospores ($14\text{--}17 \times 7\text{--}8.5 \mu\text{m}$) than the remainder of the taxa in this species complex, which feature ascospores more than 25 μm long and 10 μm broad. It is possible that only immature specimens with smaller ascospores were examined in *G. khanspurensis*. *Gyromitra korfii* and *G. ticiniana* are segregated from *G. gigas* and *G. montana*

and for ITS2 along the lower diagonal. Intraspecific variation could not be calculated for *G. khanspurensis* and *G. pseudogigas* since each species was represented by a single sequence

by narrower ascospores (10–11 μm broad in *G. korfii* and *G. ticiniana*; more than 12 μm broad in *G. gigas* and *G. montana*). Although we found no stable morphological characters to segregate *G. korfii* and *G. ticiniana*, they are geographically isolated in the eastern USA (*G. korfii*) and southern Europe/Turkey (*G. ticiniana*), respectively. *Gyromitra gigas* has longer ascospores ($L_m = 30.5\text{--}31.5 \mu\text{m}$), a higher Q_m value (2.6–2.7), and a more prominent apiculus (up to 2.5 μm long) than *G. montana* ($L_m = 27.5\text{--}29 \mu\text{m}$; $Q_m = 2.3$; inconspicuous apiculus or up to 1.0 μm long). In addition, *G. gigas* is known only from Europe and Asia whereas *G. montana* is reported only from western USA and across Canada. These differences are summarized in Table 4 and the following key to species in the *Gyromitra gigas* species complex:

Key to species in the *Gyromitra gigas* species complex

- 1. Apothecia convoluted to cerebriform.....2
- 1. Apothecia saddle-shaped; ascospores $22\text{--}31.5 \times 10\text{--}14 \mu\text{m}$; $Q_m = 2.3$; China.....*G. pseudogigas*
- 2. Ascospores more than 20 μm long and 10 μm broad; Q_m greater than 2.5.....3
- 2. Ascospores $14\text{--}17 \times 7\text{--}8.5 \mu\text{m}$; $Q_m = 1.8$; Pakistan.....*G. khanspurensis*
- 3. Ascospores 10–11 μm broad.....4
- 3. Ascospores more than 12 μm broad.....5
- 4. Eastern USA.....*G. korfii*
- 4. France, Italy, Turkey.....*G. ticiniana*
- 5. Apiculus up to 2.5 μm long; ascospores $L_m = 30.5\text{--}31.5 \mu\text{m}$, $Q_m = 2.6\text{--}2.7$; Europe and Asia.....*G. gigas*
- 5. Apiculus inconspicuous or up to 1 μm long; ascospores $L_m = 27.5\text{--}29 \mu\text{m}$; $Q_m = 2.3$; western USA and Canada.....*G. montana*

Table 4 Morphological characters, ecology and source of illustrations for the six species in the *G. gigas* species complex

Species	Ascomata shape	Ascomata color	Asci	Paraphyses	Ascospore shape	Ascospore size	Ecology	Sources of illustrations
<i>G. gigas</i> (Carbone et al. 2018)	Ascomata stipitate, 5–12 cm high; apothecium 4–11 (13) cm wide, 5–6.5 cm high, irregularly-shaped, wrinkled, contorted, margin free; stipe 4–6 × 3–5 cm, irregular, distortedly and roundly grooved, hollow.	Apothecium initially honey-yellow colored, ivory-white close to margin, then ochre, buff to rust-brown; stipe ivory, yellow to yellowish-gray.	Cylindrical, 290–330 × 19–21 µm, eight-spored, operculate, hyaline.	Cylindrical, septate, enlarged at apex up to 11 µm, filled with brown pigment in upper part.	Ellipsoid to subfusoid, sometimes inequilateral; hyaline; ornamented with low but well-defined crests which mostly form an incomplete reticulum; uniguttulate or triguttulate; with blunt, sometimes truncated apiculi up to 2.5 µm long.	(25–) 27–32 (–34.5) × (11.5–) 12–13 (–14) µm; most frequent 27–32 (–34.5) × 12–13 µm; $Q = (2.1–) 2.2–2.5$ (–2.75)	Solitary to gregarious in deciduous as well as coniferous forests or in forest clearings, often in close proximity to (or directly from) old stumps, rotten logs or other decayed wood. In central Europe it grows in woods of <i>Betula</i> or <i>Populus tremula</i> , but also in association with <i>Picea</i> , <i>Tilia</i> , <i>Carpinus</i> or <i>Quercus</i> , and occasionally other trees. <i>Gyromitra gigas</i> occurs in submontane to montane forests, on alkaline (e.g., calcareous or basaltic) and acidic (e.g., plutonic) substrates. Appearing from the second half of March until the middle of April and persisting until the beginning of May. In western and southern Europe it is mostly collected in coniferous forests (mainly <i>Picea abies</i> but also <i>Abies alba</i>) at medium to high altitude, although collectors under <i>Fagus</i> are frequently reported. In the Alps, at high elevation or after a heavy snow, it can also be found until the first half of June. In Finland and	Carbone et al. 2018

Table 4 (continued)

Species	Ascomata shape	Ascomata color	Asci	Paraphyses	Ascospore shape	Ascospore size	Ecology	Sources of illustrations
<i>G. khanspurenensis</i> (Krisai-Greilhuber et al. 2017)	Ascomata stipitate, up to 3.5 cm high; apothecium irregular, up to 2 cm high and 3.5 cm diam at widest point; stipe 3.5 × 1 cm, base slightly wider, up to 1.3 cm, smooth.	Apothecium yellowish--brown to brown; stipe off white.	Cylindric, up to 220 × 10 μm, eight-spored, operculate, hyaline.	Up to 140 × 6.5 μm, clavate, narrowing toward base; hyaline.	Ellipsoid; hyaline; smooth; guttulate; apiculus short.	14–17 × 7–8.5 μm, $Q = 1.5–2$, avg. 1.8	Norway in hemiboreal and boreal regions in May and the first half of June, most frequently in coniferous forests, rarely in deciduous forests, often in logged sites and forest borders.	Krisai-Greilhuber et al. 2017
<i>G. korffii</i> (Raitviir 1970)	Ascomata stipitate; apothecium 5–10 cm diam, irregularly lobed and plicate; stipe irregularly cylindrical.	Apothecium ochraceous--brown to brown; stipe whitish.	Cylindric, eight-spored, operculate, hyaline.	Cylindric, hyaline, with clavate, brownish apices.	Fusoid to ellipsoid-fusoid; hyaline; very finely reticulate; triguttulate; distinctly apiculate, apiculus 3–3.5 μm long.	(29.2–) 31.5–37.0 (–37.3) × (9.7–) 10.4–1–0.9 (–12) μm	Solitary to gregarious, April and May, on soil in deciduous, coniferous and mixed deciduous-coniferous forests, eastern USA (IL, KY, MA, MI, MO, NC, NY, OH, VA, WV).	Kuo 2005; Weber 1988
<i>G. montana</i> (McKnight 1971 as <i>G. gigas</i>)	Ascomata stipitate; apothecium convoluted, 5–18 cm diam; stipe 2–14 × 3–15 cm, even or expanded toward the base, longitudinally ribbed with rounded ribs, hollow.	Apothecium strong yellowish brown (near 7.5YR 5/6) to strong brown (7.5YR 4/6) or moderate brown (7.5YR 4/6); stipe white or nearly so.	Cylindric, 350–400 × 18–24 μm, eight-spored, operculate, hyaline.	Paraphyses 2–4 septate above the branches, terminal cell cylindrical--capitate, 4–12 μm diam, pale yellow in Melzer's reagent.	Ellipsoid, typically flattened on one side; hyaline; smooth or very faintly roughened with an incomplete reticulum; uniguttulate or triguttulate; apiculus lacking or very short, truncate or more often broadly rounded, 0.1–1 μm long.	(21.4–) 24.3–35.8 (–37.5) × (9–) 10.7–15.8 μm	Solitary to gregarious, May to July (depending on snowfall), on soil in coniferous or mixed deciduous-coniferous forests from the Rocky Mountains to the West Coast in USA and throughout Canada (Canada: BC, NL; USA: AZ, CA, CO, ID, MI, MT, OR, UT, WA, WY), often found around melting snowbanks and sometimes developing to	Kuo 2005; Weber 1988

Table 4 (continued)

Species	Ascomata shape	Ascomata color	Asci	Paraphyses	Ascospore shape	Ascospore size	Ecology	Sources of illustrations
<i>G. pseudogigas</i> (Wang and Zhuang 2019)	Ascomata stipitate; apothecium saddle-shaped, rugose, 1.5–3.5 cm diam and 3 cm high when dry; stipe 4 cm × 0.3–2.3 cm, subcylindric, enlarged at base, typically fluted with ribs, hollow.	Apothecium yellowish-brown to dark brown when dry; stipe yellowish-brown.	Subcylindric, 180–240 × 14–20 µm, eight-spored, operculate, hyaline.	Filiform, septate, 5.5–7 µm diam at apex, 4.5–6 µm diam below.	Ellipsoid to fusoid; hyaline; finely roughened; uniguttulate or triguttulate; apiculus, 1–4 µm long.	22–31.5 × 10–14 µm; median 27.5 × 12 µm; $Q = 1.9–2.7$, median 2.3	considerable size under snow. In China, <i>Gyromitra</i> are often collected in forests with <i>Picea</i> , <i>Pinus</i> , and <i>Betula</i> in cool and mountainous regions at altitudes of 800–4000 m, June.	Wang and Zhuang 2019
<i>G. ticiniana</i> (Carbone et al. 2018)	Ascomata stipitate, up to 11 cm high; apothecium cerebriiform, up to 8 cm wide; stipe up to 6 cm high and 7 (–9) cm diam, irregular, hollow.	Apothecium yellow-ochre then ochre, buff to rust-brown at maturity; stipe ivory, yellowish to yellowish-gray.	Cylindric, 280–300 × 18–20 µm, eight-spored, operculate, hyaline.	Cylindric, septate, enlarged at apex, up to 9.5 µm diam, filled with brown pigment in upper part.	Ellipsoid to subfusoid, sometimes inequilateral; hyaline; ornamented by low crests which form an incomplete reticulum; triguttulate; with blunt apiculi up to 2 µm long.	(22–) 25–31 × (–34) × (9.5–) 10.5–11 (–12) µm; most frequent 27–29 × 11 µm; $Q = (2.2–) 2.5–2.7$ (–2.8)	In deciduous forests on soil rich in woody remains, or close to (or directly from) old stumps or rotten logs. Seems to prefer <i>Quercus</i> spp. although a collection is reported in a pure <i>Fagus sylvatica</i> forest. <i>Gyromitra ticiniana</i> occurs from lowland to mountainous areas, up to 1000 m a.s.l., from the second half of March until May (depending on the elevation).	Carbone et al. 2018

Discussion

Three highly supported clades of sister taxa occur in the *Gyromitra gigas* species complex: *G. gigas*-*G. montana*, *G. korfii*-*G. ticiniana*, and *G. khanspurensis*-*G. pseudogigas*. For several decades, mycologists have questioned which taxonomic names to apply to North American specimens that resemble *G. gigas* (Smith 1949; Groves and Hoare 1953; McKnight 1971; Ginns 1975; Weber 1988; Abbott and Currah 1997; Kuo 2005; Methven et al. 2013; Miller et al. 2015). A search in the Mycology Collections Portal (MyCoPortal 2020) reveals that the name *Gyromitra gigas* has been applied to 281 specimens occurring in Canada and USA, whereas 197 specimens are labeled as *G. korfii* and 239 specimens as *G. montana*. Our study definitively shows that *G. gigas*, a species described from Europe, does not occur in North America and that either *G. korfii* or *G. montana* is the appropriate name to apply depending on whether material is collected in the eastern USA or western USA/Canada, respectively. Although the ascospore length and width for *G. gigas* and *G. montana* described by Carbone et al. (2018) and Harmaja (1973), respectively, overlap, the ascospores of specimens examined in this study (*G. gigas*: ILLS00121401, ILLS00121415; *G. montana*: ILLS00114753, ILLS00121414, ILLS00165101, ILLS00165152) differed in mean length ($L_m = 30.5\text{--}31.5\ \mu\text{m}$ in *G. gigas* and $27.5\text{--}29\ \mu\text{m}$ in *G. montana*) and Q_m ($2.6\text{--}2.7$ in *G. gigas* and 2.3 in *G. montana*) as well as the length of the apiculus (up to $2.5\ \mu\text{m}$ in *G. gigas* and inconspicuous or up to $1\ \mu\text{m}$ in *G. montana*). These two taxa are also geographically isolated with *G. gigas* occurring throughout Europe and Asia, whereas *G. montana* is limited to the western USA and Canada in North America. *Gyromitra korfii* and *G. ticiniana* are distinguished from *G. gigas* and *G. montana* by narrower ascospores ($10\text{--}11\ \mu\text{m}$ broad in *G. korfii* and *G. ticiniana* versus greater than $12\ \mu\text{m}$ broad in *G. gigas* and *G. montana*).

The *G. korfii*-*G. ticiniana* sister taxa relationship is intriguing since the phylogeny suggests *G. korfii* and *G. ticiniana* recently speciated (Fig. 1). This species pair displayed a small ITS barcode gap averaging 1.7% suggesting the following: (1) populations in Europe and eastern USA separated recently and interspecific variation has not yet become fixed, and/or (2) introgression is still occurring via rare dispersal events across the Atlantic not allowing the populations to completely diverge. Although the ascospores of *G. korfii* ($31.5\text{--}37 \times 10.4\text{--}10.9\ \mu\text{m}$) described by Raitviir (1970) are longer and wider than those described by Littini (1988) for *G. ticiniana* ($24\text{--}28 \times 8\text{--}10\ \mu\text{m}$), the ascospores of specimens examined in this study (*G. korfii*: CUP 58839, ILLS00114754; *G. ticiniana*: ILLS00121412, ILLS00121413) for these two taxa overlapped in length, width, Q and Q_m and could

not be used to distinguish these two taxa. Based on the non-molecular data we have assembled at this time, the only way to distinguish these two taxa (other than by DNA sequences) is geographically with *G. korfii* restricted to eastern North America and *G. ticiniana* limited to southern Europe and Turkey. Specimens of *G. ticiniana* displayed zero sequence variation in their ITS and LSU sequences even though they were sampled from three different countries (France, Italy, and Turkey). The geographical range of *G. ticiniana* overlaps with *G. gigas* so specimens collected in southern Europe and Turkey should be separated by ascospore width or sequenced for the ITS1 region to determine their identity.

Gyromitra korfii was originally described from New York, but occurs throughout the eastern USA with a range as far west as Missouri (Fig. 2). This is in contrast to *G. montana* which, except for a population in Michigan, occurs mostly in the western part of the USA and most likely throughout much of Canada. It is possible that *G. montana* prefers colder climates associated with higher elevations and higher latitudes. The Great Plains states (i.e., North Dakota, South Dakota, Nebraska, Kansas, and Oklahoma) may serve as a dividing line between *G. korfii* and *G. montana*. Only three voucher specimens (labeled as *Helvella gigas*) at NY were found to occur in Kansas (MyCoPortal 2020) and their ascospore widths should be measured or these collections should be molecularly annotated to determine their identity. Material collected in Michigan needs to be carefully examined for differences in mature ascospore widths or molecularly annotated by sequencing the ITS1 region to determine the correct name.

The third clade of sister taxa contains *G. khanspurensis*-*G. pseudogigas*. *Gyromitra khanspurensis* is distinguished from *G. pseudogigas* by the convoluted, wrinkled apothecia and smaller ascospores ($14\text{--}17 \times 7\text{--}8.5\ \mu\text{m}$; $Q = 1.5\text{--}2$; $Q_m = 1.8$) that were described as smooth with a short apiculus. *Gyromitra pseudogigas* features a saddle-shaped apothecium with larger ascospores ($22\text{--}31.5 \times 10\text{--}14\ \mu\text{m}$; $Q = 1.9\text{--}2.7$; $Q_m = 2.7$) that are finely roughened and an apiculus that is $1\text{--}4\ \mu\text{m}$ long. The small ascospores of *G. khanspurensis* and saddle-shaped apothecia of *G. pseudogigas* are unique in the *G. gigas* species complex. This species pair displayed the smallest ITS barcode gap of 0.6% (Table 2). *Gyromitra gigas* has a wide geographic distribution ranging from western Europe to eastern China where it overlaps with *G. ticiniana* and potentially overlaps with *G. khanspurensis* and *G. pseudogigas*. Additional specimens of both species need to be collected and sequenced for the ITS to better understand their geographical range and infraspecific and interspecific variation.

Acknowledgements The authors wish to thank the curators and collections managers for the loan of specimens at the following fungaria: BPI,

CUP, ILLS, LUG, O, OSC, OULU, NY, TAAM, WTU, and YSU. We also thank Andrus Voitk, Michael Kuo, and Nina Filippova for the loan of specimens.

Authors' contributions Andrew N. Miller was responsible for the study conception and design. Andrew N. Miller, Angela Yoon, and Øyvind Stensholt generated molecular sequence data. Gro Gulden, Nicolas Van Vooren, Esteri Ohenoja, and Andrew S. Methven provided voucher specimens. Molecular analyses were performed by Andrew N. Miller. Morphological analyses were performed by Andrew S. Methven. The first draft of the manuscript was written by Andrew N. Miller. Andrew S. Methven edited the manuscript and all authors commented on subsequent versions of the manuscript. All authors read and approved the final manuscript.

Data availability All data and materials have been deposited in publicly accessible holdings.

Compliance with ethical standards

Conflict of interest The authors declare that they have no conflict of interest.

Ethical approval Not applicable

Consent to participate Not applicable

Consent for publication Not applicable

References

- Abarenkov K, Tedersoo L, Nilsson RH, Vellak K, Saar I, Veldre V, Parmasto E, Proust M, Aan A, Ots M, Kurina O, Ostonen I, Jõgeva J, Halapuu S, Põldmaa K, Toots M, Truu J, Larsson KH, Kõljalg U (2010) *PlutoF*—a web based workbench for ecological and taxonomic research, with an online implementation for fungal ITS sequences. *Evol Bioinformatics Online* 6:189–196. <https://doi.org/10.4137/EBO.S6271>
- Abbott SP, Currah RS (1997) The Helvellaceae: systematic revision and occurrence in northern and northwestern North America. *Mycotaxon* 62:1–125
- Alfaro ME, Zoller S, Lutzoni F (2003) Bayes or bootstrap. A simulation study comparing the performance of Bayesian Markov chain Monte Carlo sampling and bootstrapping in assessing phylogenetic confidence. *Mol Biol Evol* 20:255–266. <https://doi.org/10.1093/molbev/msg028>
- Carbone M, Van Vooren N, Klener V, Alvarado P (2018) Preliminary phylogenetic and morphological studies in the *Gyromitra gigas* lineage (Pezizales): Epitypification of *Gyromitra gigas* and *G. ticiniana*. *Ascomycete.org* 10(5):187–199. <https://doi.org/10.25664/art-0241>
- Castresana J (2000) Selection of conserved blocks from multiple alignments for their use in phylogenetic analysis. *Mol Biol Evol* 17:540–552. <https://doi.org/10.1093/oxfordjournals.molbev.a026334>
- Darriba D, Taboada GL, Doallo R, Posada D (2012) jModelTest 2: more models, new heuristics and parallel computing. *Nat Methods* 9:772. <https://doi.org/10.1038/nmeth.2109>
- Donadini J-C (1984) Étude des discomycètes IV. Le genre *Discina* (1). *Mycol Helvet* 1(4):251–266
- Donadini J-C (1986) Le genre *Discina* (*Gyromitra*) (2). Les espèces connues – Variabilité des caractères taxonomiques – Scanning (Ascomycetes, Pezizales). *Bull Société linnéenne Prov* 38:161–187
- Gardes M, Bruns TD (1993) ITS primers with enhanced specificity for basidiomycetes - application to the identification of mycorrhizae and rusts. *Mol Ecol* 2(2):962–1083. <https://doi.org/10.1111/j.1365-294X.1993.tb00005.x>
- Ginns JH (1975) *Discina korffii*. *Fungi Candenses* 69. Biosystematics Research Institute, Ottawa
- Gouy M, Guindon S, Gascuel O (2010) SeaView version 4: a multiplatform graphical user interface for sequence alignment and phylogenetic tree building. *Mol Biol Evol* 27:221–224. <https://doi.org/10.1093/molbev/msp259>
- Groves JW, Hoare SC (1953) The Helvellaceae of the Ottawa District. *Canadian Field-Nat* 67(3):95–102
- Guindon S, Gascuel O (2003) A simple, fast and accurate algorithm to estimate large phylogenies by maximum likelihood. *Syst Biol* 52:696–704. <https://doi.org/10.1080/10635150390235520>
- Harmaja H (1969) A wider and more natural concept of the genus *Gyromitra*. *Karstenia* 9:9–12
- Harmaja H (1973) Amendments of the limits of the genera *Gyromitra* and *Pseudorhizina*, with the description of a new species, *Gyromitra montana*. *Karstenia* 13:48–58
- Hillis DM, Bull JJ (1993) An empirical test of bootstrapping as a method for assessing confidence in phylogenetic analysis. *Syst Biol* 42:182–192. <https://doi.org/10.1093/sysbio/42.2.182>
- Huelsenbeck JP, Ronquist FR (2001) MrBayes: Bayesian inference of phylogenetic trees. *Bioinformatics* 17:754–755. <https://doi.org/10.1093/bioinformatics/17.8.754>
- Huelsenbeck JP, Ronquist FR (2005) Bayesian analysis of molecular evolution using MrBayes. In: Nielsen R (ed) *Statistical methods in molecular ecology*. Springer Publishing Co, New York, pp 186–226
- Krisai-Greilhuber I, Chen Y, Jabeen S, Madrid H, Marincowitz S, Razaq A, Ševčíková H, Voglmayr H, Yazici K, Aptroot A, Aslan A, Boekhout T, Borovička J, Crous PW, Ilyas S, Jami F, Jiang Y-L, Khalid AN, Kolecka A, Konvalinková T, Norphanphoun C, Shaheen S, Wang Y, Wingfield MJ, Wu S-P, Wu Y-M, Yu J-Y (2017) Fungal systematics and evolution: FUSE 3. *Sydowia* 69:229–264. <https://doi.org/10.12905/0380.sydowia69-2017-0229>
- Krombholz JV (v) (1834) *Naturgetreue Abbildungen und Beschreibungen der essbaren, schädlichen und verdächtigen Schwämme*. Vol 3. Prag, Calve
- Kuo M (2005) *Morels*. Ann Arbor, The University of Michigan Press
- Larget B, Simon DL (1999) Markov chain Monte Carlo algorithms for the Bayesian analysis of phylogenetic trees. *Mol Biol Evol* 16(6):750–759. <https://doi.org/10.1093/oxfordjournals.molbev.a026160>
- Littini G (1988) *Gyromitra ticiniana* sp. nov. *Pagine di Botanica* 12:17–20
- McKnight KH (1968) Artifacts on spores of Discineae induced by common reagents. *Mycologia* 60(3):723–727
- McKnight KH (1969) A note on *Discina*. *Mycologia* 61(3):614–630. <https://doi.org/10.1080/00275514.1969.12018775>
- McKnight KH (1971) On two species of false morels (*Gyromitra*) in Utah. *Great Basin Nat* 31(2):35–47
- McKnight KH (1973) Two misunderstood species of *Gyromitra* (false morels) in North America. *Michigan Botanist* 12:147–162
- Methven AS, Zelski SE, Miller AN (2013) A molecular phylogenetic assessment of the genus *Gyromitra* in North America. *Mycologia* 105(5):1306–1314. <https://doi.org/10.3852/12-397>
- Miller MA, Pfeiffer W, Schwartz T (2010) Creating the CIPRES Science Gateway for inference of large phylogenetic trees. In: *Proceedings of the Gateway Computing Environments Workshop (GCE)*, 14 Nov 2010, New Orleans, Louisiana pp 1–8
- Miller AN, Matlak A, Raudabaugh D, Pärtel K, Tamm H, Methven AS, Voitk A (2015) The genus *Gyromitra* in NL. *Omphalina* 6(3):4–15
- MyCoPortal (2020) <http://mycoportal.org/portal/index.php>. Accessed on July 23
- Osmundson TW, Robert VA, Schoch CL, Baker LJ, Smith A, Robich G, Mizzan L, Garbelotto MM (2013) Filling gaps in biodiversity

- knowledge for macrofungi: contributions and assessment of an herbarium collection DNA barcode sequencing project. *PLoS One* 8(4): e62419. <https://doi.org/10.1371/journal.pone.0062419>
- Posada D, Buckley TR (2004) Model selection and model averaging in phylogenetics: advantages of Akaike information criterion and Bayesian approaches over likelihood ratio tests. *Syst Biol* 53:793–808. <https://doi.org/10.1080/10635150490522304>
- Raitviir A (1970) Once more on *Neogyromitra caroliniana*. *Botaanika-alased Tõd* 9:364–373
- Rehner SA, Samuels GL (1995) Molecular systematics of the Hypocreales: a teleomorph gene phylogeny and the status of their anamorphs. *Can J Bot* 73(Suppl 1):S816–S823
- Riva A (1998) *Gyromitra ticiniana* Litini. una specie precoce sosia macroscopico della *Gyromitra gigas*. *I Funghi* 45:37–44
- Riva A (2010) *Gyromitra littiniana* sp. nov. Descrizione di un ascomycete stipitato a crescita precoce nei boschi di latifoglie eliofile e sosia di *Gyromitra gigas*. *Schweizerische Zeitschrift für Pilzkunde* 88(6): 230–233
- Rodríguez F, Oliver JL, Marin A, Medina JR (1990) The general stochastic model of nucleotide substitutions. *J Theor Biol* 142:485–501. [https://doi.org/10.1016/s0022-5193\(05\)80104-3](https://doi.org/10.1016/s0022-5193(05)80104-3)
- Schoch CL, Seifert KA, Huhndorf S, Robert V, Spouge JL, Levesque CA, Chen W et al (2012) Nuclear ribosomal internal transcribed spacer (ITS) region as a universal DNA barcode marker for Fungi. *PNAS* 109(16):6241–6246. <https://doi.org/10.1073/pnas.1117018109>
- Smith AH (1949) *Mushrooms in their natural habitats*. Sawyer Inc, Portland
- Stamatakis A (2014) RAxML version 8: a tool for phylogenetic analysis and post-analysis of large phylogenies. *Bioinformatics* 30(9):1312–1313. <https://doi.org/10.1093/bioinformatics/btu033>
- Stamatakis A, Hoover P, Rougemont J (2008) A fast bootstrapping algorithm for the RAxML web-servers. *Syst Biol* 57:758–771. <https://doi.org/10.1080/10635150802429642>
- Swofford DL (2002) PAUP*. Phylogenetic analysis using parsimony (*and other methods). Version 4. Sinauer Associates, Sunderland
- Talavera G, Castresana J (2007) Improvement of phylogenies after removing divergent and ambiguously aligned blocks from protein sequence alignments. *Syst Biol* 56:564–577. <https://doi.org/10.1080/10635150701472164>
- Thiers B (2013) *Index Herbariorum: a global directory of public herbaria and associated staff*. New York Botanical Garden Virtual Herbarium. <http://sweetgum.nybg.org/ih>. Accessed 1 July 2020
- Van Vooren N, Moreau P-A (2009a) Essai taxinomique sur le genre *Gyromitra* Fr. *sensu lato* (Pezizales). 1. Introduction et systématique. *Ascomycete.org* 1(1):3–6. <https://doi.org/10.25664/art-0001>
- Van Vooren N, Moreau P-A (2009b) Essai taxinomique sur le genre *Gyromitra* Fr. *sensu lato* (Pezizales). 2. Le genre *Gyromitra* Fr., sous-genre *Gyromitra*. *Ascomycete.org* 1(1):7–14. <https://doi.org/10.25664/art-0002>
- Van Vooren N, Moreau P-A (2009c) Essai taxinomique sur le genre *Gyromitra* Fr. *sensu lato* (Pezizales). 3. Le genre *Gyromitra* Fr., sous-genre *Discina*. *Ascomycete.org* 1(2):3–13. <https://doi.org/10.25664/art-0003>
- Vilgalys R, Hester M (1990) Rapid identification and mapping of enzymatically amplified ribosomal DNA from several *Cryptococcus* species. *J Bacteriol* 172:4238–4246. <https://doi.org/10.1128/jb.172.8.4238-4246.1990>
- Wang X-C, Zhuang W-Y (2019) A three-locus phylogeny of *Gyromitra* (Discinaceae, Pezizales) and discovery of two cryptic species. *Mycologia* 111(1):69–77. <https://doi.org/10.1080/00275514.2018.1515456>
- Weber NS (1988) *A morel hunter's companion: a guide to the true and false morels of Michigan*. Two Peninsula Press, Lansing
- White TJ, Bruns T, Lee S, Taylor J (1990) Amplification and direct sequencing of fungal ribosomal RNA genes for phylogenetics. In: Innis MA (ed) *PCR protocols: a guide to methods and applications*. Academic Press, San Diego, pp 315–322

Publisher's note Springer Nature remains neutral with regard to jurisdictional claims in published maps and institutional affiliations.